EVALUATION OF DYNAMIC MECHANICAL PROPERTIES OF FLAX FIBER-POLYPROPYLENE (FP) COMPOSITES USING THE ADAPTIVE NEURO-FUZZY INFERENCE SYSTEM

SHETTAHALLI MANTAIAH VINU KUMAR,[*] RAVICHANDRAN ARUMUGAM THANGAVEL,[**] RANGANATHAN SOUNDARARAJAN,[*] CHANDRASEKARAN SASIKUMAR,[***] ERUSAGOUNDER SAKTHIVELMURUGAN[***] and CHINNASAMY NITHIYAPATHI[****]

[*]*Department of Mechanical Engineering, Sri Krishna College of Engineering and Technology-Kuniyamuthur, Coimbatore, Tamil Nadu, India*
[**]*Department of Mechanical Engineering, Vel Tech Rangarajan Dr Sagunthala R&D Institute of Science and Technology-Avadi, Chennai- Chennai, Tamil Nadu, India*
[***]*Department of Mechanical Engineering, Bannari Amman Institute of Technology, Sathyamangalam, Tamil Nadu, India*
[****]*Department of Aeronautical Engineering, Nehru Institute of Engineering and Technology, Coimbatore, Tamil Nadu, India*
 Corresponding author: S. M. Vinu Kumar, vinukmr1988@gmail.com

Received April 12, 2025

Flax fiber reinforced polypropylene (FP) composites were prepared using the compression moulding technique and their dynamic mechanical (DM) properties were studied based on the fiber content. Fiber loading was varied from 0 to 50 vol% with increments of 10 vol% and the samples were designated accordingly as neat PP, FP10, FP20, FP30, FP40, and FP50 composites. The results showed that increased fiber content in the PP matrix improved the DM properties, such as storage modulus (E'), loss modulus (E"), and damping factor (Tanδ). Amongst the fabricated FP laminates, FP40 composites exhibited better viscoelastic performance. Furthermore, the adaptive neuro-fuzzy inference system (ANFIS) was implemented to predict the DM properties, mainly, E' and E" of the FP composites. The validation of the ANFIS model showed that experimental and predicted results were in good agreement to each other, confirming its reliability in forecasting the DM properties of flax fiber reinforced polypropylene (FP) composites. This study also investigated the thermal degradation behavior of the FP composites using thermogravimetric analysis (TGA). The results showed that thermal stability of the neat PP improved from 432.69 °C to 463.90 °C for optimal fiber loading of 40 vol% flax fiber (FP40). Fractured samples of FP composites were examined using scanning electron microscopy (SEM) to comprehend the interfacial bonding mechanism of the FP composites.

Keywords: dynamic mechanical analysis, flax/polypropylene composites, ANFIS, woven fiber, interfacial bonding, thermogravimetric analysis

INTRODUCTION

Natural fibers are known as "ecofriendly materials" and received huge attention owing to their biodegradability, non-toxicity, plenteous availability, light weight, cost-effectiveness, sustainability, and lower energy requirements.[1,2] Therefore, natural fiber reinforced composites (NFCs) have become successful in replacing synthetic fiber reinforced composites (SFCs) in building construction, furnishings, and automobile, aeronautical and marine applications.[3] Moreover, replacing petroleum-based materials with NFCs can not only reduce the emission of carbon dioxide, but also help in lessening petroleum product usages and supplies.[4,5] Although NFCs have the potential to replace SFCs, the latter still dominates the market, because of some disadvantages of natural fibers, including their poor interfacial bonding characteristics that lead to poor mechanical properties.[1,6,7] The properties of NFCs depend on various factors, including the source of natural fiber, fiber extraction technique and treatments, fiber length, distribution and aspect ratio, fiber orientation

and/or type of weaving, matrix material, method of processing NFCs *etc*.[6,7]

Dynamic mechanical analysis (DMA) is intended to investigate the thermo-mechanical properties of the materials with respect to temperature, time, frequency and stress.[2,7] This technique typically provides insights into storage modulus, loss modulus, glass transition temperature and damping properties of the materials, collectively termed as "viscoelastic properties". As mentioned above, NFCs are employed in making various components, such as automotive parts, construction and building components, food packing products, and sports equipment.[8] For all these applications, understanding the critical DM properties of the materials is essential. For example, automotive parts should have high stiffness and resistance to mechanical stress. In the case of sports equipment, components should possess good damping property to absorb shock and vibration. Thus, the requirements for the material's properties will vary according with the application it is intended for. By comprehending viscoelastic properties, manufacturers can tailor NFCs to perform better in diverse applications.

The thermal stability of the composite is highly influenced by the fiber content. An increase in fiber loading up to the optimal weight fraction reasonably enhances the DM properties of the composites. On the other hand, increasing fiber content beyond the optimal loading would result in decreasing DM and thermal properties of the composites. Bahlouli *et al.*[9] studied the effect of fiber loading on the thermal and DM properties of *Washingtonia* fiber (WF) reinforced HDPE biocomposites. The optimal fiber loading found for maintaining thermal stability was around 20% by mass. Beyond this point, specifically at 30% loading, the melting temperature of the biocomposites decreased, indicating a reduction in thermal stability. DMA results further showed that the biocomposites with 30% WF exhibited the highest storage modulus (E) of 2211 MPa, attributed to improved stress transfer from the fiber to the matrix. Moreover, the glass transition temperature (T_g) of the biocomposites was higher than that of the HDPE matrix, signifying that the presence of fibers affects the energy dissipation characteristics of the material. Jawaid *et al.*[10] reported that the thermal stability of the kenaf fiber/bio-epoxy composite was improved with an addition of fiber loading. 50 wt% kenaf fiber composites exhibited the highest thermal stability, as evidenced by their residual and mass loss percentages. DMA results revealed the highest storage modulus (E') obtained for the 50 wt% kenaf fiber/bio-epoxy composites, indicating superior stiffness and load-bearing capacity. Sakthivelmurugan *et al.*[11] reported on the DM properties of *Alstonia macrophylla* reinforced polypropylene composite. Their study concluded that increasing the fiber content in the PP matrix enhanced the DM properties of the composites, and 40 vol% was found to be the optimum loading in the fabricated composites. Furthermore, tremendous improvements in the storage modulus (E') and loss modulus (E") of the same *Alstonia macrophylla* reinforced polypropylene composites were recorded due to the alkali treatment of the fiber.[12]

Other major directions in the research of NFCs included fiber hybridization, nano-sized reinforcement, and fiber weaving to reinforce composites. Hybrid composites exhibited superior thermo-mechanical behavior, compared to the neat laminates, as the presence of fibers restricts polymer chain mobility and enhances stress transfer.[13] This trend was observed in kenaf fiber/*Washingtonia* leaf stalk fibers reinforced epoxy biocomposites,[14] kenaf and pineapple leaf fiber reinforced phenolic composites,[15] sugar palm/kenaf fiber reinforced polypropylene.[16] Natural fibers employed in the nanoscale form within the polymer matrices could improve the viscoelastic and thermal behavior of composites. For instance, Saba *et al.*[17] showed that the addition of cellulose nanofibers into an epoxy matrix significantly improved thermal stability, with the major degradation temperature shifting to the 350–450 °C range. DMA results confirmed that E' and E" properties of the composites increased with nanofiber addition, with 0.75% CNF loading showing the highest improvement. Finally, the woven type of reinforcement has been found to overcome the major drawbacks of NFCs, ensuring uniform distribution of the fiber in both directions and providing strong interfacial adhesion.

From our literature survey, it has been found that limited works have been reported with respect to the prediction of DM properties of the NFCs. Thus, this study investigates the DM behavior of flax-reinforced polypropylene composites using ANFIS, which, to the best of the authors' knowledge, has not been reported until now. The work also includes an analysis of the thermal degradation behavior of the composites.

EXPERIMENTAL

Materials

In this investigation, flax yarns were procured from a local market and woven into irregular basket woven fabric, using a portable handloom machine, as illustrated in our previously published report.[2,3,18] M/s Ghanshyam Polyplast (Coimbatore, India) supplied the polypropylene (PP) sheets that were used as matrix material for preparing the laminates. Images of the flax woven fabric and PP sheets are shown in Figure 1, and their physico-mechanical properties are detailed in Table 1 and Table 2, respectively.

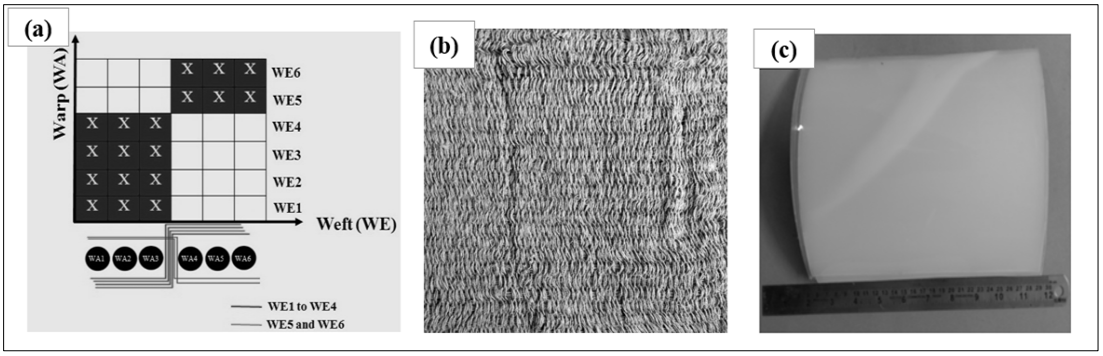

Figure 1: (a) Schematic architecture of weaving the flax fabric, (b) flax woven fabric, and (c) polypropylene sheets

Table 1
Physico-mechanical properties of flax fiber[3,7]

S.No.	Characteristic	Value	Unit
1	Cellulose	60-80	wt%
2	Hemicellulose	8-20	wt%
3	Lignin	2-5	wt%
4	Wax	1-3	wt%
5	Ash	1-2	wt%
6	Moisture	6-12	wt%
7	Density	1.4-1.5	g/cc
8	Crystalline index	60-80	%
9	Crystallite size	3-5	nm
10	Thermal stability	200-230	°C
11	Tensile strength	345-1500	MPa
12	Elongation at break	2.7-3.2	%
13	Young's modulus	27.6	GPa
14	Fiber length	10-100	mm
15	Kinetic activation energy	150-200	kJ/mol

Table 2
Physico-mechanical properties of polypropylene[11,12]

S.No.	Characteristic	Value	Unit
1	Density	0.91-0.94	g/cm^3
2	Melting temperature	160-166	°C
3	Melt flow index	3	-
4	Tensile strength	34	MPa
5	Elongation at yield	5	%
6	Flexural modulus	1310	MPa
7	Rockwell hardness, R-scale	94	-
8	Thermal conductivity	0.17	W/mK

Fabrication of FP composites

FP composites were fabricated by adopting the film stacking technique, following curing in a hot compression moulding machine. Precalculated PP sheets and flax woven fabric were stacked in an alternative sequence inside the aluminium mould and subjected to constant pressure of 25 bar with the heat supply of 180 °C from both upper and lower platens.

Curing under these conditions was maintained for 15 minutes, followed by the removal of cured laminates from the mould after cooling to room temperature. FP composites were denoted based on the fiber and matrix content in the composites. Neat PP refers to pure polypropylene, while FP10, FP20, FP30, FP40, and FP50 denote the composite material with 10, 20, 30, 40, and 50 vol% of flax fiber loading, respectively. The fabrication of the FP composites is illustrated in Figure 2 and the composition of the FP composites is provided in Table 3.

The same technique was followed for preparing all the laminates and the FP laminate thickness was uniformly maintained. As per ASTM standards of testing, the FP laminates were cut to the required dimensions for evaluating their dynamic mechanical and thermal degradation properties.

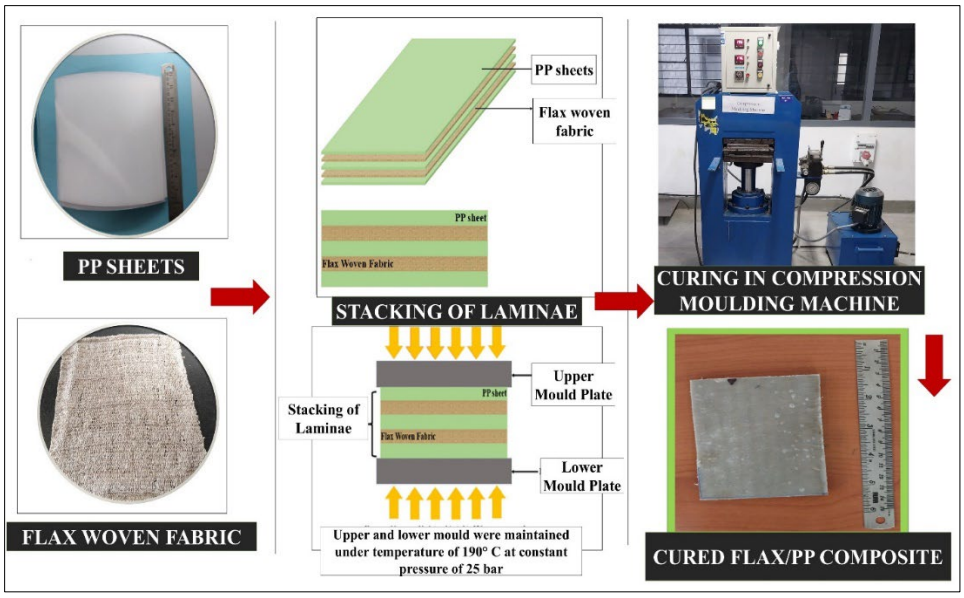

Figure 2: Processing of FP composites

Table 3
Denotation and composition of FP composites

Composite code	Laminate layers		Volume fraction (vol%)	
	Flax fiber*	PP	Flax fiber	PP
Neat PP	-	3	-	100
FP10	2	3	10±2.5	90±2.5
FP20	2	3	20±2.5	80±2.5
FP30	4	6	30±2.5	70±2.5
FP40	4	6	40±2.5	60±2.5
FP50	6	8	50±2.5	50±2.5

*Irregular basket woven fabric

Characterization methods

Dynamic mechanical analysis (DMA)

DM properties of FP composites were studied in terms of storage modulus (E'), loss modulus (E"), glass transition temperature (T_g) and damping factor (Tanδ) using a Dynamic Mechanical Analyser (SII Nanotechnology Japan-DMS 6100) in three-point bending configuration for the temperature range 25 °C–175 °C with a heating rate of 2.5 °C min^{-1} operated at a frequency 10 Hz.

ANFIS model

ANFIS was employed for prediction of storage modulus (E'), loss modulus (E") and damping (Tanδ) properties of the neat PP and FP composites. ANFIS is the combination of neural network and a fuzzy inference system. This synergy is useful to model complex and non-linear relationships, such as temperature, frequency, and viscoelastic properties of the FP composites. Moreover, ANFIS allows handling noisy and undefined experimental data, which is common in DMA studies.

This study involves only one membership function (MF) as only one input factor was considered, that is temperature. Several types of MF are available to draw the relationship between input and output variables, but in this case, the "gbellmf" type of Gaussian MF was employed and the model was developed by using MATLAB software.

ANFIS training mainly depends on MF, the number of parameters, and of fuzzy rules. During the training of the model for 500 epochs, huge variation of the RMSE value was found, irrespective of the output response chosen for different composites. This may be because, at the beginning of the training, the model's parameters were initialized randomly. Another reason may be lack of time, where the model would not minimize the cost function, but as the training progressed, increasing epochs resulted in a weaker RMSE. Similar observations were reported by other researchers,[19-21] and therefore, in this study, the ANFIS model was trained at 2000 epochs. Table 4 shows the complete details on the ANFIS used for predicting the DM properties of the neat PP and FP composites. It is clearly seen that the proposed system converged with the minimum root mean square error (RMSE) value at various ranges for different responses trained at 2000 epochs.

The Sugeno fuzzy inference system (FIS) was employed in the present study and its architecture is shown in Figure 3. Equations (1) and (2) were used to determine the performance factors for evaluating the effectiveness of the ANFIS model employed. The root means square error (RMSE) and mean absolute error (MAE) of the predicted and experimental values can be computed using Equations (1) and (2) respectively:

$$RMSE = \sqrt{\frac{\sum(j-k)^2}{m}} \quad (1)$$

$$MAE = \frac{\sum|j-k|}{m} \quad (2)$$

where m, j and k are number of patterns, the set of actual and predicted output, respectively.

The coefficient of determination (R^2) was determined for understanding the effectiveness of the mathematical model used and its value generally ranges from 0 to 1. Equation (3) was utilized for calculating the R^2 value, which gives an insight into the relationship between one term's performance and its prediction on the performance of another term.

$$R^2 = 1 - \frac{\sum(j-k)^2}{\sum(j-\bar{k})^2} \quad (3)$$

where $\bar{k}$ is the mean of the predicted output.

Thermogravimetric analysis

The thermal degradation behavior of FP composites was examined through thermogravimetric analysis (TGA) as per ASTM E1131 standards, utilizing a TGA Q 50 thermal analyzer (TA Instruments-Japan). During this test, a specimen weighing between 5-8 mg was positioned on the pan and subjected to gradual heating within an enclosed furnace, ranging from room temperature to 650 °C. The heating rate was set at 8 °C/min under a nitrogen environment. The results include the thermal degradation temperatures of both neat PP and FP composites, along with their respective residuals.

SEM analysis

The morphology of the FP composites was examined using scanning electron microscopy (SEM) (JEOL JSM-6480 LV).

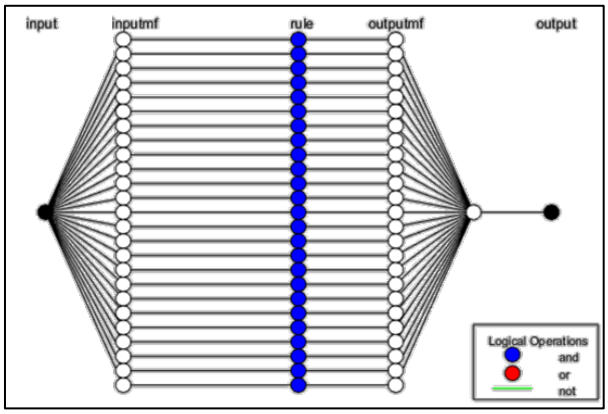

Figure 3: ANFIS architecture employed for neat PP and FP composites

Table 4
Details on the development of ANFIS predictive model for neat PP and FP composites

S. No.	Type of composites	DM property	Epochs	Membership function	Nr of nodes	Nr of linear parameters	Nr of nonlinear parameters	Total number of parameters	Nr of training data pairs	Nr of fuzzy rules	Min. training RMSE
1	Neat PP	Storage modulus (E')	2000	gbellmf	104	50	50	100	40	25	51360
	FP10		2000		116	56	56	112	66	28	119302
	FP20		2000		116	56	56	112	66	28	213025
	FP30		2000		116	56	56	112	66	28	274033
	FP40		2000		116	56	56	112	66	28	348215
	FP50		2000		116	56	56	112	66	28	276976
2	Neat PP	Loss modulus (E")	2000	gbellmf	144	70	70	140	40	35	98640
	FP10		2000		108	52	52	104	40	26	30987
	FP20		2000		108	52	52	104	40	26	67881
	FP30		2000		108	52	52	104	40	26	99067
	FP40		2000		108	52	52	104	40	26	147662
	FP50		2000		108	52	52	104	40	26	115975
3	Neat PP	Damping property (Tanδ)	2000	gbellmf	60	28	28	56	14	14	1.17E-07
	FP10		2000		80	38	38	76	19	19	1.05E-07
	FP20		2000		60	28	28	56	14	14	1.30E-07
	FP30		2000		80	38	38	76	19	19	1.41E-07
	FP40		2000		60	28	28	56	14	14	1.31E-07
	FP50		2000		80	38	38	76	19	19	0.78E-07

RESULTS AND DISCUSSION

Storage modulus of FP composites

From Figure 4, it is observed that the storage modulus (E') of the neat PP increases with an increase in the flax fiber loadings. Neat PP exhibits the E' value of 0.95 GPa, and increased to 1.01 GPa, 1.797 GPa, 2.25 GPa, 2.92 GPa, and 2.45 GPa, as the fiber loading in was increased to 10, 20, 30, 40 and 50 vol%, respectively. This enhancement in E' is mainly attributed to the mechanism of flax fiber hindering molecular chain mobility in the matrix (PP), as reported by previous researchers.[9,13] A decline of E' beyond 40 vol% of fiber loading is clearly seen, and this may be attributed to the agglomeration of fibers, though an improvement of 157.89% in the E' of FP50 was recorded compared to that of neat PP. Moreover, FP composites exhibited higher E' in the rubbery zone, as compared to the neat PP, because of the resistance caused by the flax fibers against the intense molecular mobility of the matrix material.

Loss modulus of FP composites

Figure 5 presents the loss modulus *vs.* temperature curves of neat PP and FP composites. Irrespective of the volume of fiber loadings, the E" of FP composites is found to be superior to that of neat PP. The E" of PP increases with the addition of flax fiber, and the highest value – of 0.584 GPa – was exhibited by FP40 composites, followed by FP50, FP30, FP20, and FP10. The increasing E" in the composites may be caused by the ability of the flax fiber to restrict the movement of the matrix material PP, especially during intense mobility of molecular chains. Moreover, from Figure 5, it is clearly observed that E" decreases gradually with an increase in temperature, which indicates the maximum energy dissipation would have occurred due to the intense free movement of polymer chains of the matrix material. Similarly to the situation of E', the decrease in E" beyond the optimal fiber loading is inevitable, particularly in the FP50 composite, though it exhibited superior E" values to those of neat PP and FP30 composites. However, when compared to FP40, it declined by 17.32%. This may be caused by agglomeration of the flax fiber, as a result of the plying effect, causing friction sliding between flax fibers.

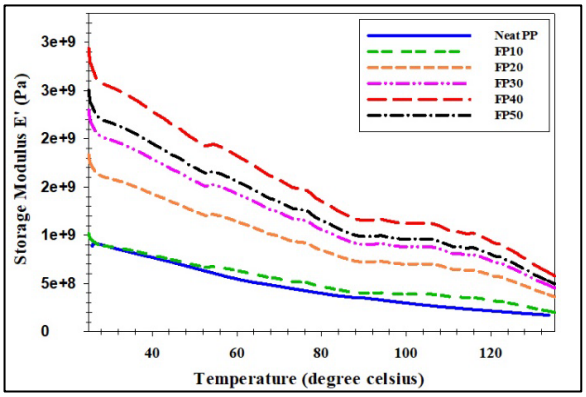

Figure 4: Storage modulus (E') curves of neat PP and FP composites for different fiber loadings

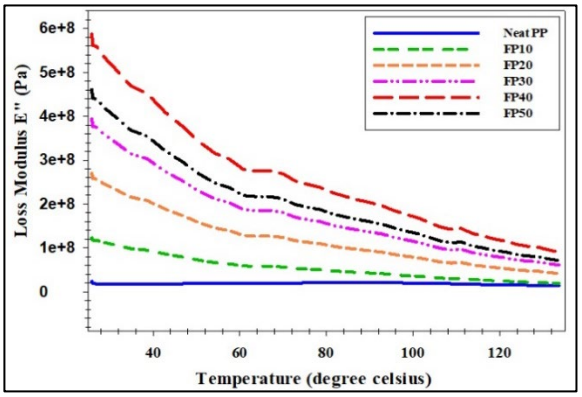

Figure 5: Loss modulus (E") curves of neat PP and FP composites for different fiber loadings

Damping of FP composites

The evolution of the damping factor of the neat PP and FP composites at different fiber loadings is shown in Figure 6. The peak height of Tanδ curves for the neat PP and FP composites is shown in Table 5. The damping peak value of the neat PP was found to be 0.11 at a temperature of 72.69 °C. From the data, it can be inferred that increasing the fiber content in FP composites results in a decrement of their damping factor value. The least damping factor, of 0.0782, was exhibited by FP40 composite, which implies that E' dominates over E" in the FP composites. This indicates that FP composites are more likely to behave in an elastic manner, having the ability to store mechanical energy with mere energy dissipation. Some researchers[9,13] indicated that a lower value of the damping factor in fiber reinforced composites was mainly due to strong interfacial bonding between the fiber and the matrix phases. This can be valid in the present investigation, where strong interfacial bonding of flax fiber and PP would facilitate a smooth transfer of mechanical load, which is pivotal in understanding the mechanical performance of the FP composites. Moreover, while enduring the transition phase, the FP

composites exhibited lower damping values due to the restriction to the molecular mobility of the polymer. With a subsequent increase in temperature, the mobility of the polymer molecular chains becomes intense, resulting in a higher damping value.

Cole-Cole plot analysis of FP composites

The relation between the storage modulus and the loss modulus of neat PP and FP composites can be observed using the Cole-Cole plot analysis, as depicted in Figure 7. The Cole-Cole plot gives an insight into changes occurring in the structural integrity of the composites, specifically after incorporating the reinforcement – the flax fiber – into PP. It is evident from the plot that the curves of FP composites broaden as the fiber loading increases. Amongst the prepared FP composites, FP40 exhibited the broadest curve, which indicates strong interfacial bonding between the flax fiber and the PP matrix, and thus the FP40 composite displayed better thermal stability than the other composites.

Table 5
Peak of Tanδ curve and EC for neat and FP composites

S. No.	Composite	Peak height of Tanδ curve	Effectiveness constant (EC)
1	Neat PP	0.1110	-
2	FP10	0.0975	0.441
3	FP20	0.0950	0.431
4	FP30	0.0926	0.424
5	FP40	0.0846	0.416
6	FP50	0.0782	0.414

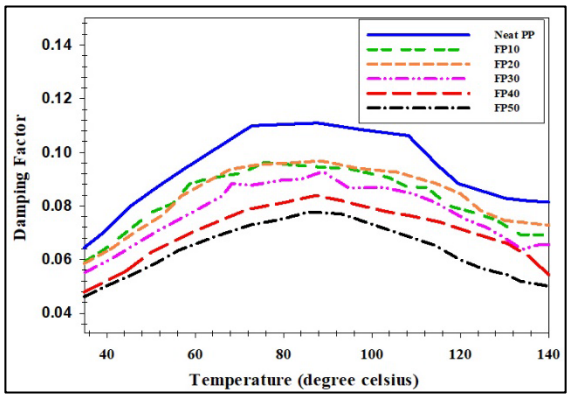

Figure 6: Damping factor curves of neat PP and FP composites for different fiber loadings

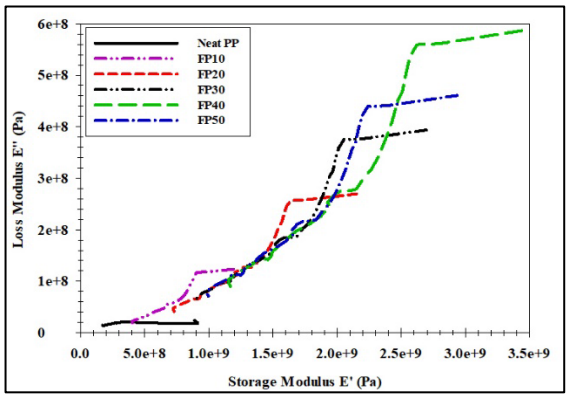

Figure 7: Cole-Cole plots of neat PP and FP composites for different fiber loadings

The effectiveness constant (EC) of the FP composites was determined and is shown in Table 5. Higher constant values of the composites indicate lower efficiency of the reinforcement phase and vice-versa. From Table 5, it can be seen that FP40 composite exhibited an EC value of 0.416, which is lower than those of the rest of the fabricated laminates, which implies that the flax fiber reinforcement in the PP matrix is effective. This can be related with the improved thermal stability of the FP40 composites due to the strong interfacial adhesion between the flax fiber and PP. Other researchers also found similar values of the effectiveness constant in fiber reinforced composites.[22,23] Kumar et *al*.[2] experimentally conducted the DMA study of flax/epoxy composites and found the EC values in the range of 0.0368 to 0.0755. Their study confirmed that 45 wt% flax fiber reinforced epoxy composites exhibited strong fiber-matrix interface, as it exhibited a lower value of EC than the rest of the flax epoxy composites. Another study carried out by Gupta *et al*.[24] confirmed that a lower EC value was exhibited by higher weight fraction reinforced jute epoxy composites due to stronger interfacial bonding.

Prediction of storage modulus (E') and loss modulus (E") using ANFIS

The prediction of storage modulus (E'), loss modulus (E"), and damping factor for neat PP and FP composites has been performed by determining the model efficiency (R. Sq. value), indicated in Table 6. It is clearly seen that the MAT error was found minimum, irrespective of the output responses: E', E" or Tanδ values, and consistent with all the classes of FP composites. Generally, the smaller the values of MAT error, the higher the accuracy of the model prediction for the given input data set, as reflected in the graph illustrated in Figure 8 and Figure 9, where ANFIS predicted data of E' and E" completely coincide with experimental data, with an accuracy of R. Sq. value of 0.9981. This kind of accuracy can be achieved only if the ANFIS model has versatility in training unseen data, which is a clear indication of the proposed model's generalization ability. A similar study was reported by Bose *et al*.,[19] who investigated the storage and loss modulus properties of the CNT based polymer nanocomposites. The authors revealed that the ability of the ANFIS model of predicting E' and E" was superior to that of ANN.

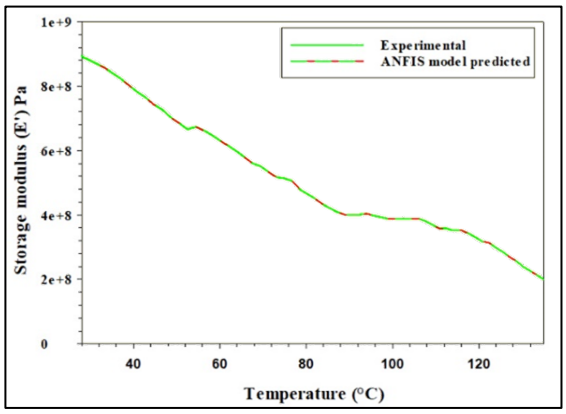

Figure 8: Experimental and ANFIS predicted results of storage modulus (E') for FP20 composites

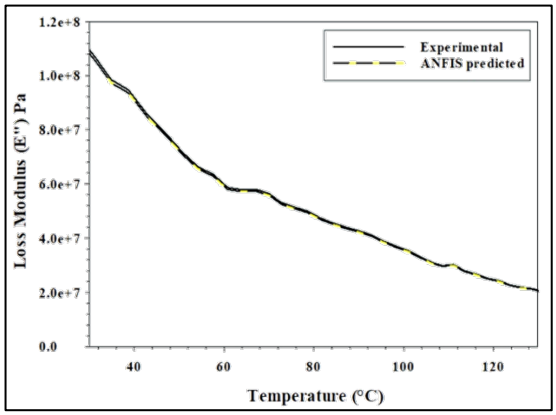

Figure 9: Experimental and ANFIS predicted results of loss modulus (E") for FP20 composites

Table 6
Information on ANFIS model for prediction of DMA properties of neat PP and FP composites

Model input	Model output	Composites	Mean absolute training (MAT) error (%)	R-Sq. value
Temperature	Storage modulus (E')	Neat PP	0.0112	0.9998
		FP10	0.0223	0.9997
		FP20	0.0214	0.9997
		FP30	0.0232	0.9997
		FP40	0.0231	0.9997
		FP50	0.0195	0.9998
Temperature	Loss modulus (E")	Neat PP	0.5299	0.9947
		FP10	0.0566	0.9994
		FP20	0.0542	0.9994
		FP30	0.0555	0.9994
		FP40	0.0497	0.9995
		FP50	0.0585	0.9994
Temperature	Damping factor (Tanδ)	Neat PP	0.0011	0.9999
		FP10	0.0110	0.9998
		FP20	0.0121	0.9998
		FP30	0.0180	0.9998
		FP40	0.0012	0.9999
		FP50	0.0144	0.9998

Thermogravimetric analysis (TGA) of FP composites

The thermal behavior of neat PP and FP composites for various fiber loadings is shown in Figure 10. As may be noted, neat PP undergoes a single-stage degradation process, with a major weight loss at the temperature of 432.69 °C. This may be attributed to the intrinsic property of the PP material, which clearly determines its degradation. However, FP composites do not exhibit any weight loss until reaching the temperature range 200-250 °C, except the FP10 composite, suggesting that 10 vol% fiber loading in the PP matrix marginally enhanced the maximum thermal degradation temperature to 437.68 °C. As it is evident from Figure 10, FP composites experience initial degradation when the temperature approaches 220 °C, which is typically related to the evaporation of moisture and other low molecular volatile matter present in the flax fiber. The samples can order by the temperature corresponding to the initial weight loss (5%) as follows: Neat PP>FP10 >FP20>FP30>FP40<FP50.

The TGA curves clearly indicate that the thermal degradation of FP composites occurred in two stages. The first stage of thermal degradation occurred in the temperature range from 220 °C to 320 °C, mainly attributed to the thermal decomposition of hemicelluloses and lignin content of the flax fiber. The second stage of decomposition is observed in the temperature range from 360 to 440 °C, which may correspond to the decomposition of PP and cellulose. A similar observation was reported by other researchers.[25,26] As the fiber loading into neat PP increases, the thermal stability of the FP composite increases, which is evident from the data in Table 7, indicating that the temperature of maximum degradation increased from 432.69 °C to 463.87 °C. This improvement may be explained by better adhesion, which could interrupt the onset of thermal degradation as the surface of the flax fiber is more stable. Subsequently, the heat transfer between flax fiber and PP matrix becomes more uniform. Apart from that, the formation of char residue plays a vital role, influencing the thermal stability of the FP composites over neat PP. This is because the char acts as a protective thermal barrier, which delays the heat transfer to the underlying PP material. Moreover, the protective layer formed by the char further insulates the FP composite from external heat, thereby the thermal stability of the FP composite enhances. The temperature that corresponds to the maximum weight loss (75%) of the samples can ordered as follows: FP40>FP50>FP30>FP20>FP10>neat PP.

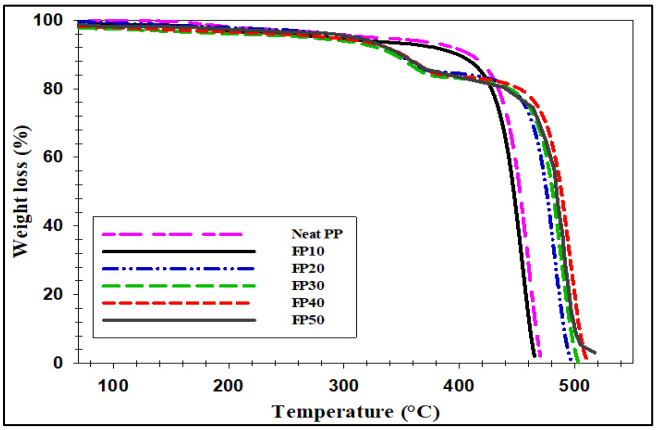

Figure 10: TGA curves of neat PP and FP composites

Table 7
Temperatures corresponding to initial and maximum weight loss of neat PP and FP composites

S. No.	Composite	Temperature (°C) of initial weight loss (5%)	Temperature (°C) of maximum weight loss (75%)
1	Neat PP	320.16	432.69
2	FP10	316.50	437.68
3	FP20	307.13	457.71
4	FP30	298.88	460.11
5	FP40	284.79	463.90
6	FP50	289.26	461.87

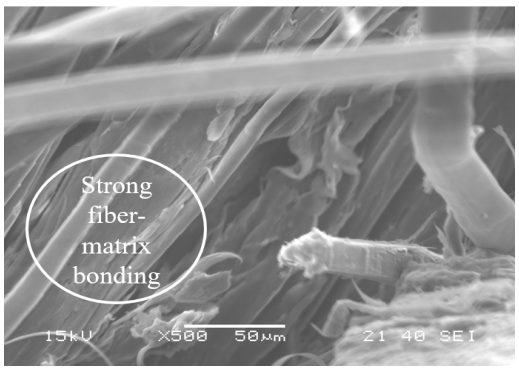

Figure 11: SEM image of the fractured surface of FP40 composite

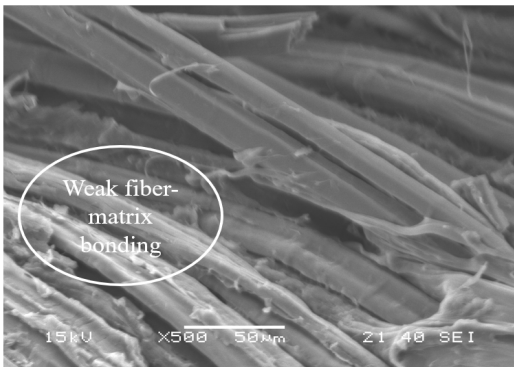

Figure 12: SEM image of the fractured surface of FP50 composite

SEM analysis

Figures 11 and 12 show the SEM images of the mechanically fractured surface of FP40 and FP50 composites. Figure 11 clearly conveys that the optimal loading of fiber in the FP40 composite ensures effective load transfer, as its fractured surface exhibits strong interfacial adhesion. Fewer voids especially at the fiber-matrix interface lead to reduced localized thermal degradation. On the other hand, Figure 12 confirms that voids and gaps in the matrix-region are quite numerous in the FP50 composite, compared to FP40. Such voids are so-called “weak spots”, as they can initiate the thermal degradation easily and diminish the mechanical properties. Agglomeration of the flax fiber is the reason for the appearance of voids in FP50 composites, and because of this, load transfer efficiency declines, making the composite unstable when exposed to high temperature.

CONCLUSION

In this study, flax-reinforced polypropylene composites were prepared and their DM properties were investigated experimentally and using ANFIS.

The storage modulus (E’), loss modulus (E”) and damping factor of the FP composite improved after incorporating the flax woven fabric into the PP matrix. Amongst the fabricated FP samples, FP40 exhibited better E’ and E”, with values of 2.92 GPa and 0.584 GPa, respectively. Higher fiber loading in FP50 composites led to lower E’ values (2.45GPa), because of the agglomeration of the flax fiber. However, when compared with the neat PP, a 157.89% improvement in E’ was still noted. This indicates the efficiency of the flax woven fabric reinforcement in the PP matrix, as confirmed by the Cole-Cole plot. TGA results showed that the thermal stability of the FP composites increased with the increase in the fiber loading, indicating the stability of flax fiber, which delayed the onset of thermal degradation.

The developed ANFIS model was found to be effective in predicting the DM properties of neat PP and FP composites as the MAT error (%) and R. Sq. value of the model were very low. The effectiveness constant (EC) of the composites was found in the range of 0.416 to 0.441. The least value was recorded by FP40 composites (0.416), which confirmed the strong interfacial adhesion between the fiber and the matrix. The same was disclosed in the SEM analysis for FP40 composites.

REFERENCES

[1] L. He, F. Xia, Y. Wang, J. Yuan, D. Chen *et al*., *Polymers* (*Basel*), **13**, 4083 (2021), https://doi.org/10.3390/polym13234083

[2] S. V. Kumar, K. S. Kumar, H. S. Jailani and G. Rajamurugan, *Mater*. *Res*. *Express*, **7**, 085302 (2020), https://doi.org/10.1088/2053-1591/abaea5

[3] V. K. Shettahalli Mantaiah, *J. Nat*. *Fibers*, **19**, 12415 (2022), https://doi.org/10.1080/15440478.2022.2060404

[4] M. Bahrami, J. Abenojar and M. Á. Martínez, *Materials*, **13**, 5145 (2020), https://doi.org/10.3390/ma13225145

[5] S. N. A. Safri, M. T. H. Sultan, M. Jawaid and K. Jayakrishna, *Compos*. *B Eng*., **133**, 112 (2018), https://doi.org/10.1016/j.compositesb.2017.09.008

[6] M. Rokbi, A. Khaldoune, M. Sanjay, P. Senthamaraikannan, A. Ati *et al*., *Int*. *J*. *Lightweight Mater*. *Manuf*., **3**, 144 (2020), https://doi.org/10.1016/j.ijlmm.2019.09.005

[7] V. K. Shettahalli Mantaiah, S. K. Kallippatti Lakshmanan and S. Kaliappagounder, *J. Nat*. *Fibers*, **19**, 10367 (2022), https://doi.org/10.1080/15440478.2021.1993504

[8] K. Ramraji, K. Rajkumar and P. Sabarinathan, *J. Mech. Eng. Sci.*, **234**, 4505 (2020), https://doi.org/10.1177/095440622092225
[9] S. Bahlouli, A. Belaadi, A. Makhlouf, H. Alshahrani, M. K. Khan *et al.*, *Polymers*, **15**, 2910 (2023), https://doi.org/10.3390/polym15132910
[10] M. Jawaid, H. A. Khalil and A. A. Bakar, *Mater. Sci. Eng. A*, **527**, 7944 (2010), https://doi.org/10.1016/j.msea.2010.09.005
[11] E. Sakthivelmurugan, G. Senthil Kumar, S. Vinu Kumar and H. Singh, *J. Braz. Soc. Mech. Sci. Eng.*, **45**, 400 (2023), https://doi.org/10.1007/s40430-023-04339-y
[12] E. Sakthivelmurugan, G. Senthil Kumar and S. V. Kumar, *Mater. Res.*, **26**, e20230108 (2023), https://doi.org/10.1590/1980-5373-MR-2023-0108
[13] M. Jawaid, S. Awad, A. S. Ismail, M. Hashem, H. Fouad *et al.*, *J. Therm. Anal. Calorim.*, **149**, 10441 (2024), https://doi.org/10.1007/s10973-024-13017-7
[14] M. B. Alshammari, A. Ahmad, M. Jawaid and S. A. Awad, *J. Mater. Res. Technol.*, **25**, 1642 (2023), https://doi.org/10.1016/j.jmrt.2023.06.035
[15] M. Asim, M. Jawaid, M. T. Paridah, N. Saba, M. Nasir *et al.*, *Polym. Compos.*, **40**, 3814 (2019), https://doi.org/10.1002/pc.25240
[16] S. Mohd Izwan, S. Sapuan, M. Zuhri and A. Mohamed, *Polymers*, **13**, 2961 (2021), https://doi.org/10.3390/polym13172961
[17] N. Saba, A. Safwan, M. Sanyang, F. Mohammad, M. Pervaiz *et al.*, *Int. J. Biol. Macromol.*, **102**, 822 (2017), https://doi.org/10.1016/j.ijbiomac.2017.04.074
[18] C. Sasikumar, E. Sakthivelmurugan and J. Rishi, *Mater. Technol.*, **55**, 851 (2021), https://doi.org/10.17222/mit.2021.256
[19] S. Bose, D. Shome and C. Das, *Int. J. Ind. Syst. Eng.*, **6**, 207 (2010), https://doi.org/10.1504/IJISE.2010.034337
[20] S. M. V. Kumar, R. Jeyakumar, N. Manikandaprabu and C. Sasikumar, *Cellulose Chem. Technol.*, **58**, 833 (2024), https://doi.org/10.35812/CelluloseChemTechnol.2024.58.74
[21] S. M. Vinu Kumar, N. Manikandaprabu, N. Babu and C. Sasikumar, *Cellulose Chem. Technol.*, **58**, 101 (2024), https://doi.org/10.35812/CelluloseChemTechnol.2024.58.10
[22] P. Krishnasamy, G. Rajamurugan and M. Thirumurugan, *J. Ind. Text.*, **51**, 6884S (2022), https://doi.org/10.1177/1528083720935570
[23] T. Sathishkumar, *J. Mater. Des. Appl.*, **230**, 160 (2016), https://doi.org/10.1177/1464420714552
[24] M. Gupta and R. Srivastava, *Indian J. Fibre Text.*, **47**, 64 (2017)
[25] S. V. Kumar and H. Singh, *Indian J. Fibre Text.*, **48**, 326 (2023), https://doi.org/10.56042/ijftr.v48i3.6057
[26] S. M. V. Kumar, J. Rengaraj and E. Sakthivelmurugan, *Cellulose Chem. Technol.*, **58**, 547 (2024), https://doi.org/10.35812/CelluloseChemTechnol.2024.58.51